EPJ Web of Conferences **96**, 01011 (2015)
DOI: 10.1051/epjconf/ 20159601011

Status of the KLOE-2 experiment

Alessandro Di Cicco[1,2,a] on behalf of the KLOE-2 Collaboration

[1] *Roma Tre University, Mathematics and Physics Department, Rome, Italy*
[2] *INFN Roma Tre, Rome, Italy*

Abstract. The KLOE-2 experiment at the Frascati National Laboratory of the INFN is undergoing commissioning, together with the e^+e^- collider DAΦNE.
The KLOE apparatus, consisting of a huge Drift Chamber and an Electromagnetic Colorimeter working in a 0.5 T axial magnetic field, has been upgraded with the insertion of an Inner Tracker, two low-angle calorimeters (CCALT and QCALT) and low-angle taggers (LET and HET) for $\gamma\gamma$−physics.
Cosmic-ray muon and collision data are being acquired in order to optimize the sub-detectors operation in view of the new data taking campaign. The first results from the ongoing commissioning of the KLOE-2 detector will be shown.

1 Introduction

The KLOE-2 experiment at the Frascati National Laboratory (LNF) of the INFN is undergoing commissioning, together with the e^+e^- collider DAΦNE. The KLOE-2 project aims at improving the successful and fruitful results achieved by the KLOE Collaboration [1] and extending its physics program to $\gamma\gamma$−physics, searches of hidden-sector dark matter particles, neutral-kaon interferometry, CPT and Quantum Mechanics tests, rare kaon decays, CKM matrix elements constraints and lepton flavor violation, light hadron spectroscopy and hadron cross-section at low energy. The KLOE-2 physics program [2] will be performed thanks to the recent DAΦNE collider and KLOE detector upgrades.

DAΦNE is the e^+e^- collider of the Frascati Laboratory, working at a centre-of-mass energy equal to the ϕ−meson mass. DAΦNE delivered 2.5 fb^{-1} on-peak and 250 pb^{-1} off-peak integrated luminosity to the KLOE experiment.

The KLOE experiment consists of a huge Drift Chamber (DC) [3], providing high-momentum resolution ($\sigma_p/p = 0.4\%$) on reconstructed tracks, and a Pb-scintillating fibers calorimeter (EMC) [4], with excellent time ($\sigma_t = 54\,ps/\sqrt{E(GeV)} \oplus 140\,ps$) and good energy ($\sigma_E/E = 5.7\%/\sqrt{E(GeV)}$) resolutions, both working in a 0.5 T axial magnetic field. In fig. 1 a vertical cross-section of the KLOE apparatus along the beam line is showed. The DC provides a 3-dimensional reconstruction of tracks exploiting its stereo-geometry and fills almost uniformly the whole detector volume. The EMC has barrel and end-cap modules which allow to cover 98% of a solid angle. A superconductive coil provides the 0.5 T magnetic field.

DAΦNE is currently providing collisions, with background rates ≤ 400 kHz. The machine operation parameters are being optimized to further reduce the background level.

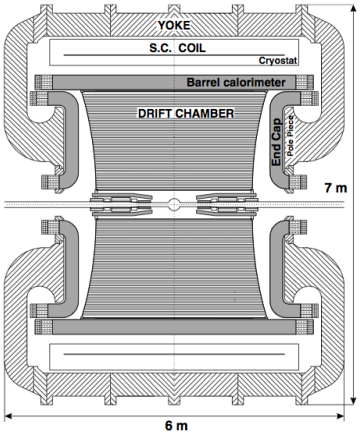

Figure 1. Vertical cross-section of the KLOE detector along the beam line.

Along with the Drift Chamber and the Electromagnetic Calorimeter, new calorimeters and a tracking device have been installed inside the KLOE detector to improve detection and reconstruction performance of particles produced very close to the interaction region.

The KLOE apparatus has been upgraded with the insertion of an Inner Tracker, two low-angle calorimeters (CCALT and QCALT) and low-angle taggers (LET and HET) for $\gamma\gamma$−physics. The Inner Tracker has been installed between the interaction region and the Drift Chamber inner wall in order to improve vertex reconstruction and small-angle coverage. The tracking device consists of four co-axial and cylindrical triple-GEM layers, which allow us to keep the material budget below 2% of the radi-

[a] e-mail: alessandro.dicicco@roma3.infn.it

ation length (X_0), as required in order to minimize multiple scattering of low-momentum tracks and to reduce low-energy photons conversion. The LET is a calorimeter made up of LYSO crystals read out by SiPMs. It has been installed inside the KLOE interaction region. The HET is a plastic-scintillator-based calorimeter read out by scintillating fibers. It has been installed along the beam pipe. The CCALT is a calorimeter composed of LYSO crystals read out by APDs; it has been inserted around the interaction region together with the Inner Tracker. The QCALT is a calorimeter made up of plastic-scintillator tiles and absorbing material sandwiches, whose light is collected by wavelength shifters and read out by SiPMs. This detector has been installed on the permanent quadrupoles of the DAΦNE collider. All the sub-detectors are being commissioned using cosmic-ray muons and collision data.

In the following sections the KLOE-2 sub-detectors will be described and their status reported.

2 The KLOE-2 detector

A Low Energy Tagger (LET) [5] and a High Energy Tagger (HET) [6] have been installed with the aim of detecting electrons and positrons originating from $e^+e^- \to e^+e^-\gamma^*\gamma^* \to e^+e^-X$ reactions. A Quadrupole Calorimeter with Tiles (QCALT) [7] has been installed on the DAΦNE permanent quadrupoles to ensure coverage for K_L decays. A Crystal Calorimeter with Timing (CCALT) [8] has been installed very close to the interaction point (IP), in order to increase the acceptance for photons coming from the IP. An innovative fully-cylindrical GEM detector – the Inner Tracker (IT) [9] – has been installed around the IP in order to achieve better vertex reconstruction performance for low-momentum tracks coming from the IP.

A more detailed description of all the new sub-detectors will be found in the following paragraphs.

2.1 The $\gamma\gamma$ taggers

The new tagging stations of the KLOE-2 apparatus will be used to detect electrons/positrons scattered in $\gamma\gamma$ interactions. Most of the scattered e^+e^- are emitted in the forward directions and, since their energy is below 510 MeV, they deviate from the equilibrium orbit during the propagation along the machine lattice. Therefore a tagging system must consists of more than one detector located in well identified regions along the beam line, aimed to determine the energy of the scattered electrons either directly or from the measurement of their displacement from the main orbit.

Two identical low-energy tagging calorimeters have been placed symmetrically at 1 m at both sides of the IP (fig. 2), in order to tag electrons/positrons with energy 160 < E < 400 MeV and a mean angle of 11° with respect to the beam axis. This inner detector is referred to as LET. It exploits a 20 Cerium doped Lutetium Yttrium Orthosilicate (LYSO) crystal-scintillator $6 \times 7.5 \times 12$ cm^3 matrix, singly readout by Silicon Photomultipliers (SiPM) photodetectors. The energy resolution is $\sigma_E/E < 10\%$ for

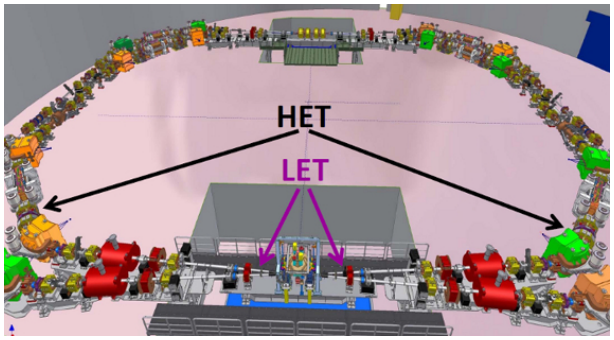

Figure 2. HET and LET positions along the beam line. The LET calorimeters are placed at both sides of the interaction point and are enclosed in the KLOE apparatus volume. The HET calorimeters are placed at both sides of the interaction point, but outside the KLOE volume.

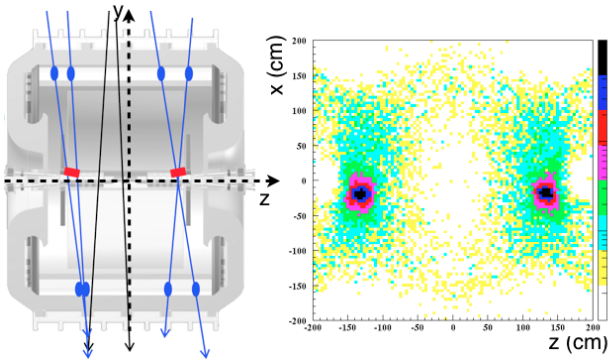

Figure 3. *Left*: Red boxes represent the two LET stations fired by cosmic-ray muon tracks, displayed as solid blue lines. Tracks are selected by requiring two energy depositions in the barrel EMC with E > 5 GeV and at least one LET crystal fired, z, y axes are reported (dashed arrows). *Right*: Positions of the let stations in the $x - z$ plane as measured by using selected muon tracks.

electrons/positrons of energy E > 150 MeV, while the time resolution is $\sigma_t \sim 1$ ns.New front-end electronic boards and ADCs have been produced for the LET detectors to improve rate capability. High-energy cosmic-ray muons crossing the LET are being used to equalize the detector response, calibrating position and energy measurements. In fig. 3 reconstructed positions of the LET stations in the $x - z$ plane are displayed (right), together with the experimental setup used for calibration (left).

Detection of scattered electrons/positrons with energy in the range 400-500 MeV is provided by another tagging station, the HET. Two identical calorimeters have been placed at both side of the IP, at 11 m along the beam line (fig. 2). The HET stations consist of 30 small $3\times3\times5$ mm^3 plastic scintillator, whose light is brought by light guides to readout Photomultipliers (PMT). The plastic scintillator arrangement provides a 2.5 MeV energy and a 200 ps time resolutions. New front-end electronic boards have been exploited to make possible HET operation in low-noise conditions. The HET calorimeters are clearly able to solve the $\sim$ 2.7 ns bunch-spacing time-structure when

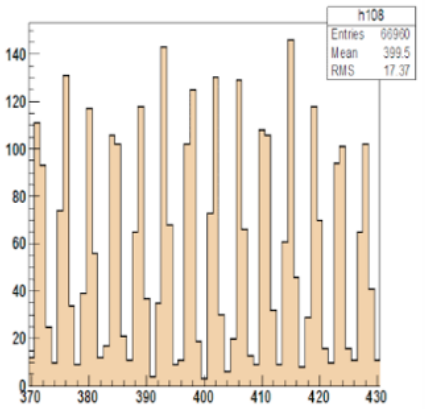

Figure 4. Bunch structure in TDC counts as seen by one HET station. The detector time resolution is good enough to disentangle the bunch spacing. This is a measurement performed by illuminating the HET station with an electron beam at the Frascati Beam Test Facility.

electrons circulate in DAΦNE as shown in fig. 4, in which a measurement performed by illuminating the HET station with an electron beam at the Frascati Beam Test Facility is reported.

2.2 The tile and crystal calorimeters

Two new tile calorimeters, QCALT, have been installed around the DAΦNE quadrupoles, at both sides of the IP, with the goal of improving the reconstruction of photons originating from K_L neutral decays and hitting the quadrupoles. Each calorimeter consists in a dodecagonal structure (fig. 5), 1 m long, surrounding the quadrupoles. The structure is arranged as a sampling of 5 layers of 5 mm-thick scintillator plates alternated with 3.5 mm-thick tungsten plates, for a total $\sim 5\,X_0$. The active part of each plane is divided into 20 tiles of 5×5 cm ^{2} area with 1 mm diameter wavelength shifter fibers embedded in circular grooves. Each fiber is then optically connected to a SiPM, for a total of 2400 channels. The QCALT is characterized by a $\sigma_z \sim 2\,mm$ resolution on the z-coordinate (along the beam axis) and a $\sigma_t \sim 1\,ns$ time resolution. A multi-engine cooling system has been recently used to reduce front-end electronics temperature. Both QCALT modules have been switched on and equalized. Some occupancy plots for one module are reported in fig. 6 as example.

In order to increase acceptance for photons coming from $\eta-$meson and rare K_S decays down to 11°, few crystals have been installed between the IP and the focalizing quadrupoles. The CCALT detectors, placed at both sides of the IP, are made up of $2 \times 2 \times 13$ cm^3 special-shaped LYSO crystals (fig. 7), arranged in a dodecagonal structure, readout by Avalanche Photodiodes (APD). The LYSO crystals well match the request of high efficiency to low energy photons and excellent time resolution for the CCALT, which will help in rejecting machine background events in the low-energy region. A $\sigma_E/E = 5\%$ at $E = 500\,MeV$ energy resolution and a $\sigma_t \sim 49\,ps$ at $E = 100\,MeV$ time resolution have been measured for CCALT crystals with tests performed at the Frascati Beam Test Facility. The time resolution measured with E = q00 MeV electrons is reported in fig. 8.

Figure 5. *Left*: QCALT dodecagonal structure with the LET housing in evidence. *Right*: QCALT structure with front-end cables in evidence.

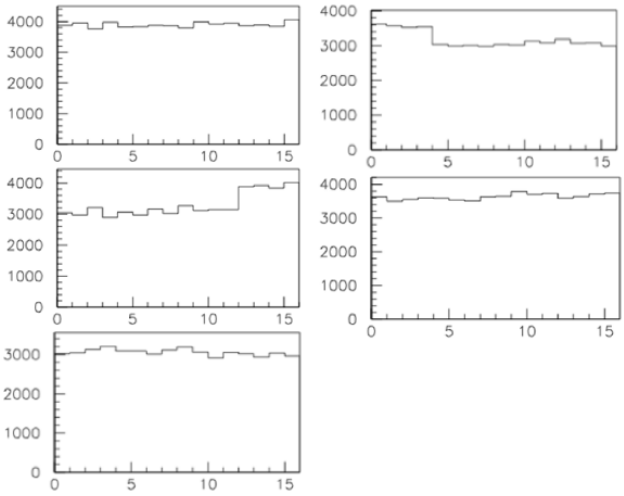

Figure 6. Occupancy plots for one module of the QCALT calorimeter. All the module channels are on and equalized as showed.

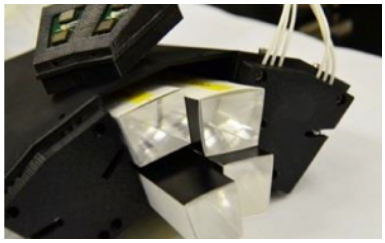

Figure 7. Some special-shaped CCALT LYSO crystals in their housing structure.

2.3 The Inner Tracker

The Inner Tracker detector is composed of 4 cylindrical triple-GEM coaxial layers, each equipped with a double-view XV-strips/pads readout circuit. A picture of the tracker before its installation around the KLOE interaction region is reported in fig. 9. The dimension of the

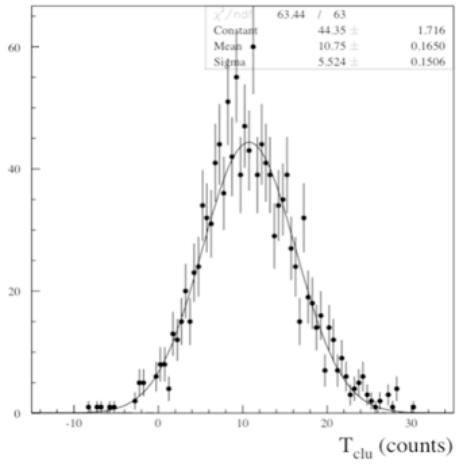

Figure 8. Time resolution measurement performed illuminating the CCALT crystals with 100 MeV electrons at the Frascati Beam Test Facility.

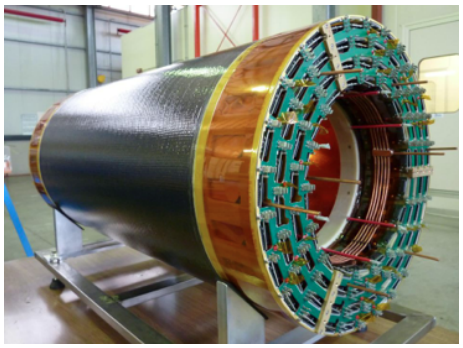

Figure 9. A picture of the Inner Tracker before its installation inside the KLOE interaction region.

active area ($\sim$ $700 \times 300\,mm^2$) required the GEM deliverer (CERN TE-MPE-EM workshop), in collaboration with INFN-LNF groups, to proceed with a new manufacturing technique [10], while the assembly procedure has been totally developed at LNF.

The Inner Tracker has been installed between the beam pipe and the DC inner wall. The high-rate capability of GEM detectors made possible to place the IT very close to the interaction point, thus improving the resolution of K_S decay points located within a few cm from the IP. An accurate study showed that an improvement on this resolution of a factor ~ 3 could be reached. The overall material budget of the IT is only $\sim$ 0.2% of X_0. This is important because multiple-scattering contribution to track resolution and photon conversion before the DC volume must be minimized.

Although each layer has been tested in a dedicated area at LNF, before their integration in the IT, new tests with the detector in its final position are required. Inner Tracker must be aligned and calibrated in order to get the best tracking performance. Efficiency extraction must also be performed in order to optimize the tracker working point. Optimization of operational conditions is ongoing

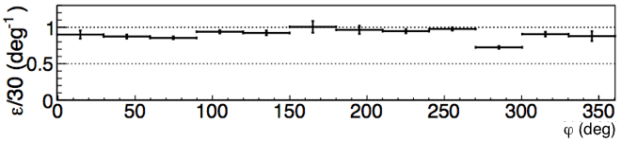

Figure 10. Inner Tracker efficiency as a function of the $\varphi-$angle in the bending plane for one of the IT layers.

and tools to monitor the detector and measure its efficiency have been developed, together with alibration and alignment procedures exploiting cosmic-ray muon and Bhabha-scattering events. Fig. 10 shows the present efficiency measured for one IT layer. Efficiency is evaluated by selecting tracks reconstructed by the DC and crossing the IT at two points. After evaluating the expected crossing positions, measured clusters on the IT are reconstructed. Then, the efficiency is computed as the ratio between measured and expected position distributions, as a function of the $\varphi-$angle in the bending plane. The low efficiency values in some of the $\varphi-$regions are correlated to the presence of dead and/or noisy strips.

3 Conclusions

The KLOE experiment has been upgraded and all sub-detectors are undergoing commissioning together with the DAΦNE collider. A data-taking period has started and data are being acquired with all detectors included. Drift Chamber and Electromagnetic Calorimeter have been calibrated as well as HET and LET calorimeters. For the new sub-detectors the optimization of operational parameters together with their calibration is going to be concluded.

4 Acknowledgements

We warmly thank our former KLOE colleagues for the access to the data collected during the KLOE data taking campaign. We thank the DAΦNE team for their efforts in maintaining low background running conditions and their collaboration during all data taking. We want to thank our technical staff: G.F. Fortugno and F. Sborzacchi for their dedication in ensuring efficient operation of the KLOE computing facilities; M. Anelli for his continuous attention to the gas system and detector safety; A. Balla, M. Gatta, G. Corradi and G. Papalino for electronics maintenance; M. Santoni, G. Paoluzzi and R. Rosellini for general detector support; C. Piscitelli for his help during major maintenance periods. This work was supported in part by the EU Integrated Infrastructure Initiative Hadron Physics Project under contract number RII3-CT- 2004-506078; by the European Commission under the 7th Framework Programme through the 'Research Infrastructures' action of the 'Capacities' Programme, Call: FP7-INFRASTRUCTURES-2008-1, Grant Agreement No. 227431; by the Polish National Science Centre through the Grants No. DEC-2011/03/N/ST2/02641, 2011/01/D/ST2/00748, 2011/03/N/ST2/02652, 2013/08/-M/ST2/00323, and by the Foundation for Polish Science

through the MPD programme and the project HOMING PLUS BIS/2011-4/3.

References

[1] F. Bossi *et al.*, Riv. Nuovo Cimento Vol. **31** n. 10 (2008).

[2] G. Amelino-Camelia *et al.*, Eur. Phys. J. C**68**, 619 (2010) [arXiv:1003.3868 [hep-ex]].

[3] M. Adinolfi *et al.*, Nucl. Instr. Meth. A**488**, 51 (2002)

[4] M. Adinolfi *et al.*, Nucl. Instr. Meth. A**482**, 364 (2002)

[5] D. Babusci *et al.*, Nucl. Instr. Meth. A**617**, 81 (2010)

[6] F. Archilli *et al.*, Nucl. Instr. Meth. A**617**, 266 (2010)

[7] M. Cordelli *et al.*, Nucl. Instr. Meth. A**617**, 105 (2010)

[8] F. Happacher *et al.*, Nucl. Phys. B**197** 215 (2009)

[9] A. Balla *et al.*, Nucl. Instr. Meth. A**628**, 194 (2011)

[10] M. Alfonsi *et al.*, Nucl. Instr. Meth. A**604**, 23 (2009)